La mer 36: 91–100, 1999
Société franco-japonaise d'océanographie, Tokyo

Numerical experiments of inertial oscillations in the Kuroshio, west of Okinawa

Kye-Young KIM* and Jong Yul CHUNG*

Abstract: NAKAJIMA *et al.* (1994) reported that inertial oscillations were generated in the Kuroshio, west of Okinawa by the typhoon in August and September, 1990 and that they were found at the underlying region of the Kuroshio as well as the surface Ekman layer. To simulate observed inertial currents and to investigate the main factors controlling the temporal and spatial structures of inertial oscillations, numerical modelings with ideal and real wind forcing were carried out, separately. According to the numerical results of ideal forcing, inertial oscillations are mainly controlled by the temporal variation of wind and mean flow. As the mean flow becomes stronger, inertial oscillations tend to be weakened. Temporal variation of the wind is very important as well because it is closely related with addition or removal of momentum generated by surface stress. In addition, the way of representing the turbulent process is important in simulation of inertial oscillations.

Numerical results with real wind forcing showed discrepancy with the observed inertial currents (NAKAJIMA *et al.*, 1994). Compared with the observed results, it has small amplitudes of inertial currents and large phase differences. This inconsistency seems to be derived from the various factors such as stratification, mean flow, wind data and characteristics of numerical model. It also suggests that simulation of the vertical structure of inertial oscillations is impractical.

1. Introduction

Inertial oscillations have been widely observed in the ocean and they are known to be produced by sudden changes of the surface wind stress associated with the local wind field, passage of a hurricane, sea breeze and interaction of the barotropic tide with bottom topography (CHEN *et al*, 1996). The wind-generated inertial oscillations are observed to be intensified near the surface and reduced as the mixed layer deeper (GILL, 1982). They transfer kinetic energy downward and make the mixed layer deepen (MELLOR and DURBIN, 1975 ; KLEIN, 1980 ; MARTIN, 1985 ; SHAY *et al.*, 1992 ; TROWBRIGE, 1992). Sometimes, the inertial energy can oscillate the deep water through the thermocline (KROLL, 1975 ; NOWLIN *et al.*, 1986; NAKAJIMA *et al.*, 1994).

To examine the factors determining temporal and spatial structures of inertial oscillations, numerical modelings have been performed by several investigators. Using one-dimensional model, POLLARD (1970) generated inertial waves by winds. He suggested that the amount of energy put into inertial oscillation is nearly independent of the stratification and of the horizontal scale of the wind but is strongly influenced by the temporal variation of the wind. Also, he pointed out that the changes in the wind field are very important in both generating and destroying inertial oscillations. KLEIN (1980) simulated the deepening of the mixed layer generated by inertial oscillations and reported that the thermal and dynamic structure of the marine upper layers are affected by the periodicity of the wind sequences as well as the wind forcing. Similarly, CHEN *et al.* (1996) related the generation of inertial oscillations with the temporal variation of the surface wind stress. They reported that a simple mixed layer model, when the downward transfer of the near-inertial energy to the deep stratified layer is small, shows agreement with the near-inertial currents in the mixed layer.

On the contrary, according to the results of

* Department of Oceanography, Seoul National University, Seoul 151-742, Korea.

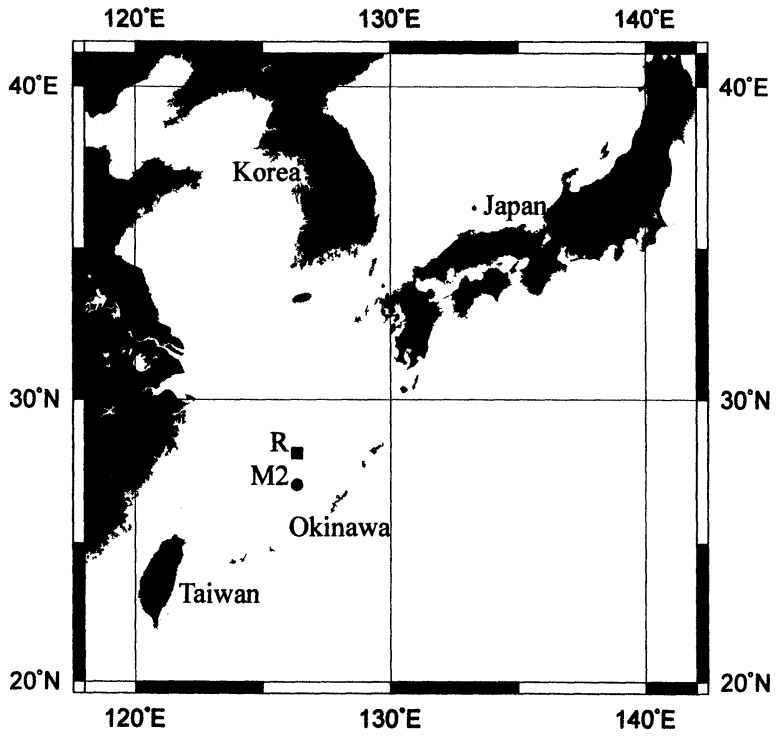

Fig. 1. Locations of the ADCP mooring (M2) and JMA buoy (R) (NAKAJIMA *et al.*, 1994). The location of M2 is 27°04′ N, 126°21′ E and that of R is 28°10′ N, 126°20′ E. The depth of station M2 is about 1500 m and the depth of the moored ADCP is 398 m in August and September, 1990. The sampling interval of M2 is 30 minutes and it was recorded at 16 m intervals. The wind at R was measured at 8 m height above the sea surface every 3 hours.

two-dimensional numerical model in a recent paper (CHEN and XIE, 1997), the cross-self gradient of surface elevation and the vertical gradient of Reynolds stress control the inertial oscillations. While the temporal and spatial structures of inertial oscillations in the open ocean depend on the local wind field, thickness of the mixed layer and vertical stratification, they are constrained by the coastline and are modified due to the bottom topography in the coastal region (CHEN *et al.*, 1996).

Recent studies about inertial oscillation in the Kuroshio mainly introduced their generations by typhoons (TAIRA *et al.*, 1993; NAKAJIMA *et al.*, 1994; TAKANO *et al.*, 1994; MAEDA *et al.*, 1996). Especially, NAKAJIMA *et al.* (1994) analyzed one-year term moored ADCP data obtained in the Kuroshio west of Okinawa and explained inertial oscillations in relation with the wind data of Japan Meteorology Agency (JMA) buoy robot (Fig. 1). They reported that strong inertial oscillations were observed not only in the surface Ekman layer but also in the underlying region of the Kuroshio during the typhoon period and that they were also accompanied by significant reduction of the Kuroshio energy at the surface layer.

The purpose of this study is to examine the important factors mentioned above for the generation of inertial oscillations using a numerical model and to simulate the inertial oscillations with the observed values of NAKAJIMA *et al.* (1994)

2. Numerical Model

The model used in this study is the Princeton Ocean Model (POM) developed by BLUMBERG and MELLOR (1987). It uses a sigma coordinate

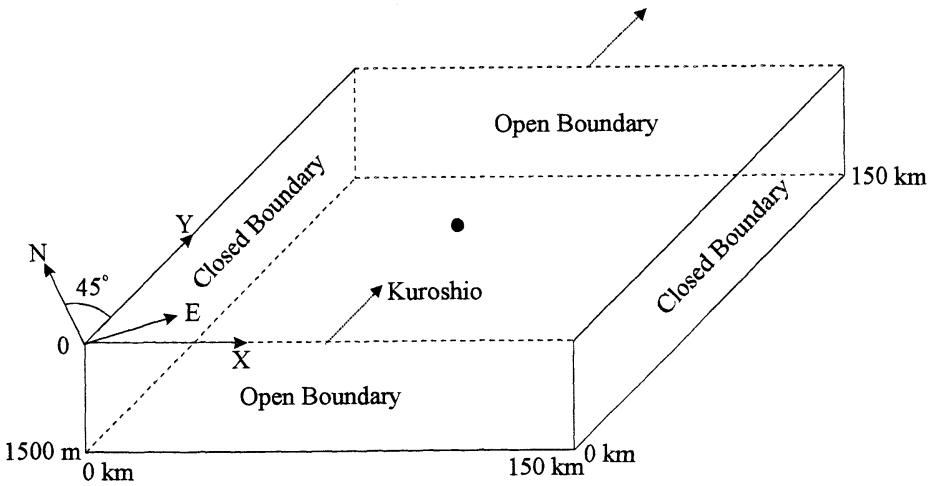

Fig. 2. Schematic of the structure of the numerical model; The solid circle indicates the location of computed velocities shown in Fig. 5 and 6.

in the vertical direction and a Cartesian coordinate in the horizontal directions. It has a "mode splitting" technique to calculate the external mode and internal mode separately.

The model consists of the continuity, momentum, hydrostatic, temperature and density equations :

$$u_x+v_y+w_z=0 \tag{1}$$

$$u_t+uu_x+vu_y+wu_z-fv = -p_0^{-1}p_x+(K_Mu_z)_z+F^u, \tag{2}$$

$$v_t+uv_x+vv_y+wv_z+fu = -p_0^{-1}p_y+(K_Mv_z)_z+F^v, \tag{3}$$

$$pg=-p_z, \tag{4}$$

$$T_t+uT_x+vT_y+wT_z=(K_HT_z)_z+F^T, \tag{5}$$

$$S_t+uS_x+vS_y+wS_z=(K_HS_z)_z+F^S, \tag{6}$$

$$p=p(T,S) \tag{7}$$

Where (u, v, w) are the velocity components in the (x, y, z) directions, respectively; P is the pressure; T is the temperature; S is the salinity; p is *in situ* density; p_0(=constant) is the reference density; f is the Coriolis parameter; g is the gravitational acceleration; K_M is the vertical eddy viscosity; K_H is the vertical eddy diffusivity; $F^{(u,v)}$ is the horizontal eddy friction terms; and $F^{(T,S)}$ is the horizontal eddy diffusion terms. The equations of (1)-(6) are transformed into the sigma coordinate system defined by $\sigma=(z-\eta)/(H+\eta)$, where η and H are the surface elevation and the water depth, respectively.

The horizontal viscosity coefficient A_M and A_H are set to 500 m^2/s and the vertical eddy viscosity and diffusion coefficients are calculated from the level 2.5 turbulent kinetic energy closure (MELLOR and YAMADA, 1982). For simplicity, frictional coefficients are assumed to be constant in time; $C_z=0.0025$.

The model domain is a rectangular basin of constant depth 1500 m, of which x and y-axis are 45° rotated clockwise from the north (Fig. 2). The northern and southern boundaries are opened to consider the Kuroshio. The grid spacing is 5 km at the x and y-direction, respectively and it has a distance of 150 km and a width of 150 km. To compare with the ADCP observations described by NAKAJIMA *et al.* (1994), $\Delta\sigma=0.011$ of vertical spacing is used above 395 m and $\Delta\sigma=0.033$ was used between 395 m and 1500 m (49 points in the vertical). According to the typical CFL condition given by BLUMBERG and MELLOR (1987), the external time step used in this study is 12 seconds and the internal time step is 180 seconds.

The numerical experiments were run with ideal and real wind forcing, separately. In case of ideal wind forcing (Table 1), the basic distribution of temperature was given by a simple equation (Fig. 3a),

$$T=5.0+25.0\times e^{H/350} \tag{8}$$

Table 1. Summary of the numerical experiments in case of ideal wing forcing ; T, temperature ; K_M, vertical eddy viscosity ; K_H, vertical eddy diffusivity ; W_S, wind speed in Eq. 9 ; Wd, direction of wind blowing ; V_{mean}, mean flow in the v-direction ; ΔT, internal time step : M-Y, level 2.5 turbulent kinetic energy closure (MELLOR and YAMADA, 1982),

Experiment	T (℃)	K_M and K_H	W_S (m/sec)	Wd	V_{mean} (m/sec)	ΔT (sec)	Description
1	Eq. 8	M-Y	20	South	0.0	180	Basic case
2	20	M-Y	20	South	0.0	180	Homogeneous
3	Eq. 8	M-Y	20	South	0.0	180	Weak stratified ($T=5.0+12.5xe^{H/350}$)
4	Eq. 8	0.001	20	South	0.0	180	$K_M=K_H=0.001m^2/s$
5	Eq. 8	0.01	20	South	0.0	180	$K_M=K_H=0.01m^2/s$
6	Eq. 8	M-Y	30	South	0.0	180	Strong Wind
7	Eq. 8	M-Y	20	West	0.0	180	Constant wind
8	Eq. 8	M-Y	20	West	0.0	180	Different direction of wind blowing
9	Eq. 8	M-Y	20	South	0.1	180	Mean flow of 0.1 m/s
10	Eq. 8	M-Y	20	South	0.2	180	Mean flow of 0.2 m/s
11	Eq. 8	M-Y	20	West	0.2	180	Experiment 8+Mean flow of 0.2 m/sec
12	Eq. 8	M-Y	20	South	0.0	540	Large internal time step

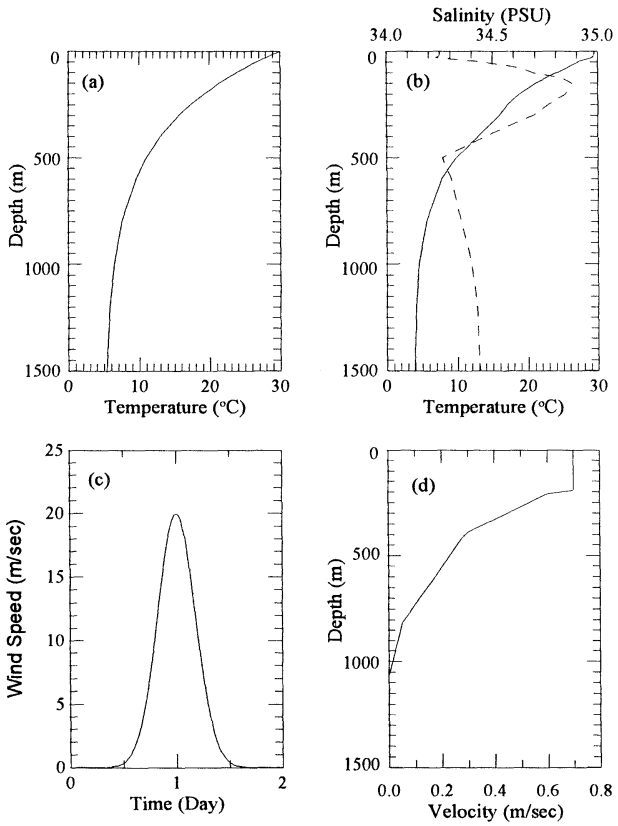

Fig. 3. Initial distribution of (a) temperature in case of ideal wind forcing, (b) temperature (thick line) and salinity (dashed line) in case of real wind forcing, (c) ideal wind speed (d) mean flow in the direction of Kuroshio in case of real wind forcing.

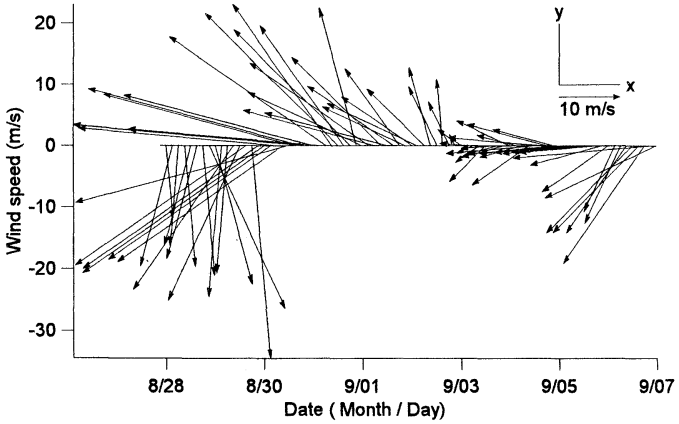

Fig. 4. Wind vectors of a JMA buoy robot (No.22001) at R station in Fig. 1 during August 28 to September 7, 1990 when the typhoon T9015 passed the site.

where H is the water depth and salinity was set to 35 psu. On the contrary, in case of real wind forcing, the initial distribution of temperature and salinity was given by a vertical profile of observed data from NODC oceanographic database. The sampling location is 27° 00′ 00″ N, 126° 22′ 59″ E and the sampling date is July 28, 1990 (Fig. 3b).

In case of ideal wind forcing, the form of Gaussian function is used (CHEN and XIE, 1997), i.e.,

$$W = W_S e^{-\frac{(t-a)^2}{b^2}} \tag{9}$$

where W_S is the amplitude of the wind velocity, a is a time of the maximum wind and b is the e -folding time scale. In our experiments, a was taken as 24 hours and b was 6 hours (Fig. 3c). The data of real wind was taken from a buoy robot (No. 22001) of the JMA during the same period of the ADCP mooring (Fig. 4).

For most of the experiments, free radiation condition was used, while the external and internal velocities were specified at the open boundaries in some cases (Table. 1). In case of real wind forcing, the flow field of Kuroshio was taken from the velocity distribution during autumn in 1991 (YUAN *et al.*, 1994) and it was imposed at the open boundaries (Fig. 3d).

According to NAKAJIMA *et al.* (1994), the inertial period at the station M2 is 26.3 h and hence, to compare with the ADCP observations, the band-passed filter admitting periods between 25 and 30 hours was used in calculating inertial currents. After the wind blowing stopped (Fig. 3c), the model was run for 5 days in cases of ideal wind forcing. for real wind forcing, the model was run for 10 days except the spin-up time.

3. Model Results and Discussion

Numerical experiments of ideal wind forcing were carried out to study the dependence of the response on stratification, vertical eddy viscosity and diffusivity, wind speed, wind direction, mean current and numerical time step (Table 1).

The effect of stratification was examined by stratified and homogeneous cases. Experiment 1 (Fig. 5a) shows the basic case of model response to the wind stress, caused by the wind pattern of Fig. 3c. The amplitudes of the inertial currents at the upper layer above 50 m were greater than 0.3 m/s and it gradually decreased when water depth increased. On the contrary, in homogeneous case, near-inertial currents are very weak and they decayed rapidly after the wind stopped (Fig. 5b). In addition, the oscillations in the upper layer were almost in phase with the lower layer, while they were 180° out of phase in stratified case (Fig. 5a). The effect of reduced stratification is shown in Fig. 5c and it seems that the downward transfer of energy from the upper layer

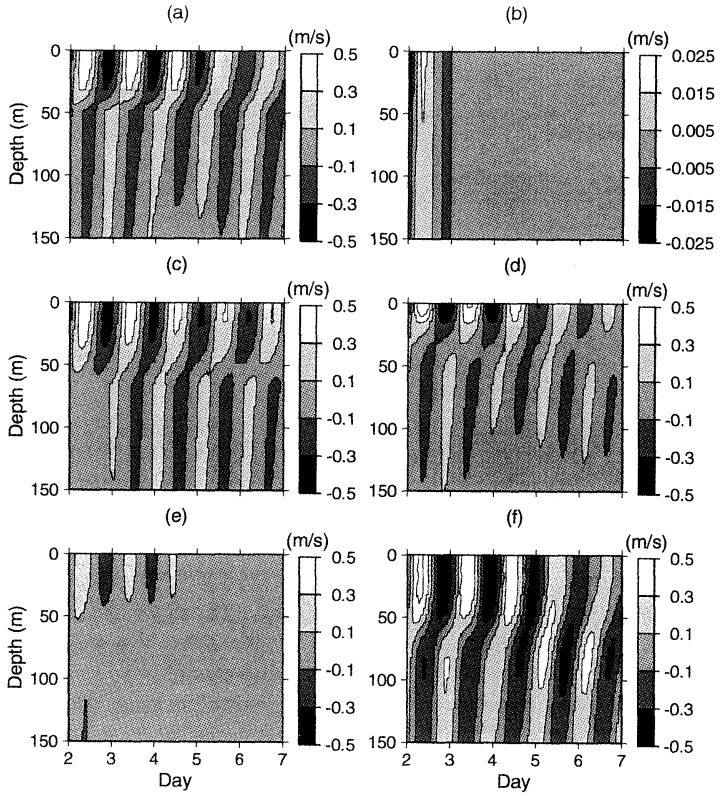

Fig. 5. Time series of the band-passed inertial currents at the surface layer of Fig. 2 from (a) experiment 1 with a basic stratified case, (b) experiment 2 with a homogeneous case, (c) experiment 3 with a weak stratified case, (d) experiment 4 with $K_M=K_H=0.001$ m^2/s, (e) experiment 5 with $K_M=K_H=0.01m^2/s$, and (f) experiment 6 with strong wind. The contour represents the v-velocity.

was more active than that of experiment 1. It coincides with the result of POLLARD (1970) that the stratification controlled the rate at which energy at near-inertial frequencies dispersed downwards out of the forced layer.

Experiment 4 and 5 shows the effects of different parameters for vertical eddy viscosity and diffusivity. According to the result of experiment 4 with constant vertical eddy viscosity and diffusivity, $K_M=K_H=0.001$ m^2/s, sharp gradients of inertial currents appear at the upper layer and rapidly decay as time goes on (Fig. 5d). Velocities of experiment 4 are stronger than those of experiment 1 during only few hours after wind had stopped. On the other hand, in experiment 5 with $K_M=K_H=0.01$ m^2/s, inertial oscillations are very weak (Fig. 5e). ALLEN *et al.* (1995), in the numerical simulation of the upwelling circulation at Oregon continental shelf with different parameterizations for vertical eddy viscosity and diffusivity, pointed out that the across-shelf circulation with constant coefficients differs considerably from that in the basic case with the MELLOR-YAMADA level 2.5 closure. Similarly, our results of experiment 4 and 5 show the importance of the particular representation of turbulent processes used in the model and it implies that the simulation of inertial currents with real wind field can be very difficult.

Effects of different wind speed and duration are shown in Fig. 5f and 5g. In experiment 6 of the strong wind case, the inertial velocities are stronger than those of experiment 1 and the

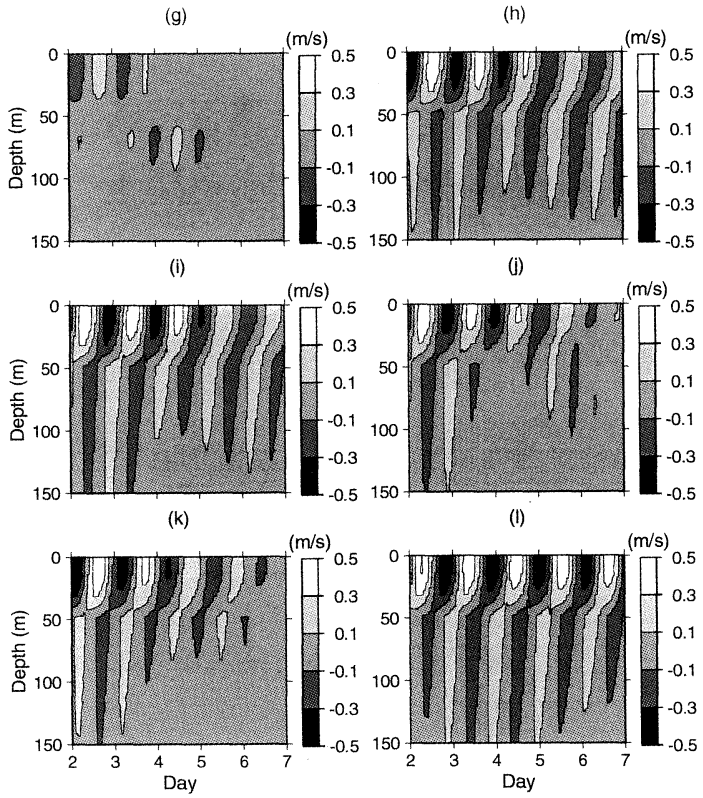

Fig. 5. (Continued)(g) experiment 7 with constant wind, (h) experiment 8 with westward wind (i) experiment 9 with mean flow, $V_{mean}=0.1m/s$, (j) experiment 10 with mean flow, $V_{mean}=0.2m/s$, (k) experiment 11 with mean flow, $V_{mean}=0.2m/s$ and westward wind and (l) experiment 12 with large internal time step.

downward transfer of energy seems to be more effective (Fig. 5f). However, in experiment 7 of constant wind blowing instead of impulsive wind forcing, the inertial velocities are very weak (Fig. 5g), which clearly shows that inertial oscillation is strongly influenced by the time dependence of wind blowing (POLLARD, 1970). The duration of wind blowing is the important factor in determining whether the momentum will be added or removed from the oscillations.

When wind is blowing westward, the vertical distribution of v-velocity is similar to that of experiment 1 (Fog. 5h). However, if numerical experiments of inertial oscillations were run in shallower regions with varying depths, it would be dependent on the direction of the wind (CHEN and XIE, 1997).

When a mean current of 0.1 m/s exists, inertial oscillations become weaker than those of experiment 1 (Fig. 5i). In experiment 10, a mean current 0.2 m/s is used and inertial currents become much weaker (Fig. 5j). Similarly, when the wind is blowing westward and the mean current of 0.2 m/s exists (Fig. 5k), amplitudes of inertial currents are smaller than those of experiment 8 (Fig. 5h). According to CHEN and XIE (1997), when the wind phase was opposite of diurnal tidal currents, the interaction of wind- and tide-induced currents tends to reduce the amplitude of near-inertial oscillations. In our experiments, even though there is no diurnal tidal current, the mean current plays a role in reducing the amplitude of inertial current.

In experiment 12, of which numerical time

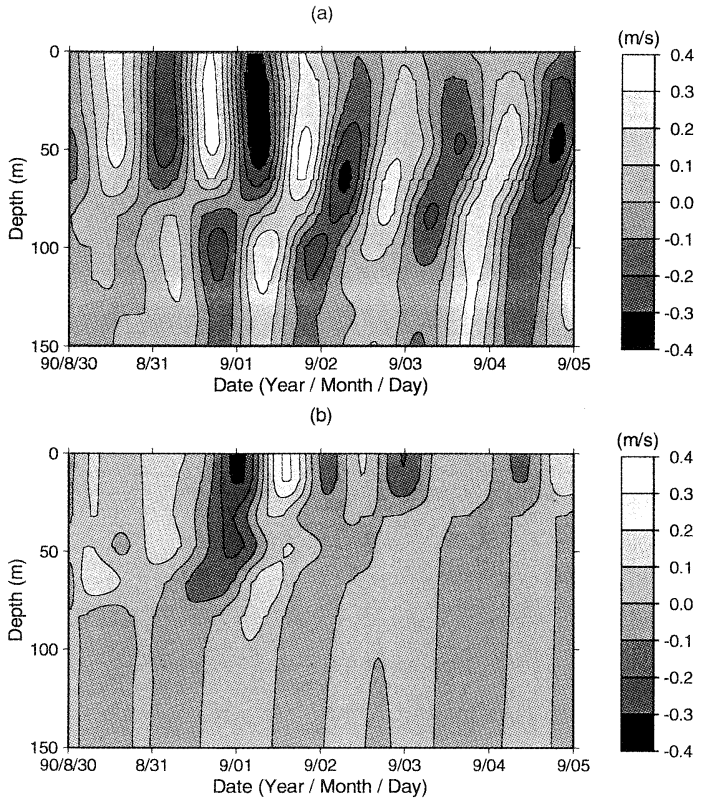

Fig. 6. Time series of the band-passed inertial currents at the depth from 0 to 150 m of Fig. 2 from (a) observed ADCP velocities (b) calculated velocities with real wind forcing between August 28 and September 7, 1990. The contour represents the v-velocity.

step is three times of experiment 1, the vertical distribution of inertial currents become stronger (Fig. 5l). This result shows that the simulation of inertial oscillation is not so simple. In our experiments, three-dimensional velocities were calculated at every internal time step and the same profile of wind stress (Fig. 3c) as experiment 1 was used. However, different amplitudes of inertial oscilations were generated simply because the time interval of calculating three-dimensional velocities was defferent from that of experiment 1. The result seems to be strange at first sight, but it was proved by GILL (1982) using a simple equation that the amplitude of inertial oscillation is strongly dependent on the time of the wind variation.

Figure 6a represents the near-inertial currents observed from a moored ADCP during a typhoon attacked the station M2 (Fig. 1) in August and September, 1990 and the downward propagation of inertial oscillations is well expressed. As expected from our previous numerical experiments of ideal wind forcing, numerical results with real wind forcing are in poor agreement with the observed (Fig. 6b). The amplitudes of inertial currents are relatively small and they have large phase differences with the observed ones. In addition, downward propagation of inertial oscillations seems to be hindered after September 2, 1990. The reasons for this poor result can be considered as follows.

First, as pointed out by ALLEN *et al.* (1995), the representation of turbulent processes used in the numerical model is important. When a wind stress begins to act on the surface of a stratified fluid, momentum is mixed rapidly

downwards by turbulence to create a well-mixed layer. Additionally, when the mixed layer is very weakly stratified, momentum is spread fairly evenly through it (POLLARD, 1970). As shown in our results of experiment 2 and 3 (Fig. 5b and 5c), the effect of stratification on the downward transfer of momentum cannot be ignored. In addition, the initial distribution of temperature and salinity (Fig. 3b) may not be appropriate to the simulation because the sampling location and period is not exactly the same as those of the ADCP mooring site. However, it is clear that the selection of parameters like vertical eddy viscosity and diffusivity is more important in turbulent process (Fig. 5d and 5e). In Princeton Ocean Model (POM) used in this study, vertical eddy viscosity and diffusivity are calculated using the level 2.5 turbulent kinetic energy closure (MELLOR and YAMADA, 1982) and ALLEN *et al.* (1995) reported that the results of simulation with constant coefficients differed considerably from that with this turbulence model. Moreover, MARTIN (1985) pointed out that the calculated mixed layer depths are too shallow in this turbulence model. Therefore, it can be concluded that simulation of inertial oscillation with real wind forcing is dependent on the characteristics of numerical model itself.

Secondly, because of the temporal variation of wind, the simulation of inertial currents has limits on representing not only its vertical structure but also its surface layer. As presented in the results of the experiments 6 and 7, it is natural that increase of wind speed (Fig. 5f) and the duration of wind (Fig. 5g) are the important factors in determining inertial oscillations. However, the result of experiment 12 with different numerical time step confirms that the amplitude of inertial oscillation is strongly dependent on the time of the wind change. It also implies that comparisons of simulated inertial oscillations with the observed are impractical. In addition, the location of wind buoy, which is about 100 km apart from that of the ADCP mooring, can be one of the reasons for poor results. It appears that the 3-hour interval in measuring wind is too long to apply it to numerical modeling.

4. Conclusion

Inertial oscillations in the open ocean are mainly controlled by the temporal variation of the wind, mean flow and stratification. In the generation of inertial oscillations, stratification plays a role in controlling the rate at which energy is transferred downwards out of the forced layer, but the temporal variation of the wind and the mean flow are more effective in controlling its rate. As the mean flow strengthens, inertial oscillations tend to weaken and they are almost independent of wind directions. The temporal change of the wind is closely related with addition or removal of momentum generated by surface stress and it is more important than any other factors in determining the generation of inertial oscillations. In addition, the way of representing the turbulent process is very important in simulation of the inertial oscillations. Numerical experiments with constant vertical eddy coefficient show the considerable differences from the case with the MELLOR-YAMADA level 2.5 closure. It is because the transfer of the momentum from the upper layer is calculated with the vertical eddy coefficient in numerical modeling.

Numerical results with real wind forcing show discrepancy with the observed results. The calculated amplitudes of inertial currents were relatively small and showed large phase differences with the observed. This appears to result from the combined effects of all parameters such as stratification, mean flow, wind data and characteristics of numerical model. Furthermore, it clearly shows that it is impractical and difficult to simulate the vertical structure of inertial oscillations with real wind forcing and to compare it with the observed.

Acknowledgements

The authors would like to thank Professor NAKAJIMA and Professor KANEKO of Hiroshima University for providing the moored ADCP data obtained in the Kuroshio, west of Okinawa.

References

ALLEN, J. S., P. A. NEWBERGER and J. FEDERIUK (1995): Upwelling circulation on the Oregon continental

shelf. Part I : Response to idealized forcing. J. Phys. Oceanogr., **25**, 1843–1866.

BLUMBERG, A. F. and G. L. MELLOR (1987): A description of a three-dimensional coastal ocean circulation model. In three-dimensional coastal ocean models, Coastal Estuarine Sci., **4**, 1–16.

CHEN, C., R. O. REID and W. D. NOWLIN JR. (1966): Near inertial oscillations over the Texas-Lousiana shelf. J. Geophys. Res., **101**, 3509–3524.

CHEN, C. and L. XIE (1997): A numerical study of wind-induced, near-inertial oscillations over the Texas-Lousiana shelf. J. Geophys. Res., **102**, 15583 15593.

GILL, A. E. (1982): Atmosphere-Ocean Dynamics. Academic Press, New York, 662pp.

Japan Meteorological Agency (1990): Data from ocean data buoy stations, **14**.

KLEIN, P. (1980): A simulation of the effects of air-sea transfer variability on the structure of marine upper layers. J. Phys. Oceanogr., **10**, 1824–1841.

KROLL, J. (1975): The propagation of wind-generated inertial oscillations from the surface into the deep ocean. J. Mar. Res., **33**, 15–51.

MAEDA, A., K. UEJIMA, T. YAMASHIRO, M. SAKURAI, H. ICHIKAWA, M. CHAEN, K. TAIRA and S. MIZUNO (1996): Near inertial motion excited by wind change in a margin of the typhoon 9019. J. Oceanogr., **52**, 375–388.

MARTIN, P. (1985): Simulation of the Mixed Layer at OWS November and Papa with several models. J. Geophys. Res., **90**, 903–916.

MELLOR, G. L. and P. A. DURBIN (1975): The structure of the ocean surface mixed layer. J. Phys. Oceanogr., **5**, 718–728.

MELLOR, G. L. and T. YAMADA (1982): Development of turbulence closure model for geophysical fluid problems. Rev. Geophys. Space Phys., **20**, 851–875.

NAKAJIMA, H., S. HAHIMOTO, A. KANEKO, K. KAWATATE and S. MIZUNO (1994): Inertial oscillations at the Kurushio west of Okinawa. La mer, **32**, 261–269.

NOWLIN, W. D., Jr., J. S. BOTTERO and R. D. PILLSBURY (1986): Observation of internal and near-inertial oscillations at Drake Passage. J. Phys. Oceanogr., **16**, 87–108.

POLLARD, R. T. (1970): On the generetion by winds of internal waves in the ocean. Deep-Sea Res., **17**, 795–812.

POLLARD, R. T. and R. C. MILLARD, JR. (1970). Comparison between observed and simulated wind-generated inertial oscillations. Deep-Sea Res., **17**, 813–821.

SHAY, L. K., P. G. BLACK, A. MARIANO and D. HAWKINS (1992): Upper ocean response to hurricane Gilbert. J. Geophys. Res., **97**, 20227–20248.

TAIRA, K., S. KITAGAWA, H. OTOBE and T. ASAI (1993): Observation of temperature and velocity from a surface buoy moored in the Shikoku Basin (OMLET-88). J. Oceanogr., **49**, 397–406.

TAKANO, K., Y. YUAN, K. KAWATATE, S. IMAWAKI, J. Su, Z. Pan, H. ICHIKAWA and S. UMATANI (1994): Diurnal and semidiurnal current fluctuations at abyssal depths southeast of Okinawa. La mer. **32**, 251–259.

TROWBRIDGE, J. H. (1992): A simple description of the deepening and structure of a stably stratified flow driven by a surface stress. J. Geophys. Res., **97**, 15529–15543.

Received Octover 14, 1998
Accepted January 13, 1999